

Enhanced Radiation Property of Triangular Antenna and Tuning Stub

A.Sanjeevi kumar^{#1}, Dr.A.Rajalingam^{#2}, V.Prabu^{#3}

^{#1}Research scholar CMJ University, India

^{#2}Professor Saveetha University, India

^{#3}Asst.Professor Veltech Multitech Engineering College. India.

¹s_ayyanar@yahoo.com

²dr.a.rajalingam gmail.com

³prabucvj@gmail.com

Abstract—Microstrip antennas are widely used in various applications because of low profile, low cost, lightweight and conveniently to be integrated with RF devices, here the technologies used to reduce surface waves is using Electromagnetic Band Gap (EBG) or photonic band gap structure (PBG). Recently introduction of EBG and DGS (Defected Ground Structure) made a significant break-through in the improvement of microstrip antennas characteristics. This paper discusses the influence of hexagonal shape DGS towards the improvement of the radiation properties.

I. INTRODUCTION

Microstrip antennas are widely used in various applications because of low profile, low cost, lightweight and conveniently to be integrated with RF devices. However, microstrip antennas have also disadvantages. One disadvantage is the excitation of surface waves that occurs in the substrate layer. Surface waves are undesired because when a patch antenna radiates, a portion of total available radiated power becomes trapped along the surface of the substrate. It can extract total available power for radiation to space wave. Therefore, surface wave can reduce the antenna efficiency, gain and bandwidth. For arrays, surface waves have a significant impact on the mutual coupling between array elements. One solution to reduce surface waves is using electromagnetic band gap (EBG) or photonic band gap structure (PBG). Recently introduction of EBG and DGS made a significant break-through in the improvement of microstrip antennas characteristics. EBG are a new type of engineered materials with periodic structures that can control the propagation of electromagnetic waves to an extent that was previously not possible. However, in implementing EBG, a large area is needed to implement the periodic patterns and it is also difficult to define the unit element of EBG. Whereas DGS has similar microwave circuit properties as EBG, it can also modify guided wave properties to provide a band pass or band stop like filter and can easily define the unit element. DGS is realized by etching the ground plane of microstrip antenna, this disturbs the shield current distribution in the ground plane which influences the input impedance and

current flow of the antenna. The geometry of DGS can be one or few etched structure which is simpler and does not need a large area to implement it.

Many shapes of DGS slot have been studied for single element microstrip antenna such as circle, dumbbells and spiral, however not many have realized it in antenna arrays. In [1], they proposed using a dumbbell EBG structure and in [2] using a fork-like EBG structure. Both references implemented EBG between two element arrays, these antenna designs are complex structure. The author found papers by Salehi et al. [3] and by Zainud-Deen et al. [4] which used dumbbell shape DGS for antenna array, however the results were simulation one and not realized through experimental results.

In an antenna array, the mutual coupling effect will deteriorate the radiation properties of the array. Therefore in this study, the reduction of the mutual coupling effect was investigated by proposing a new hexagonal shape DGS to be implemented between the two elements triangular patch microstrip antenna array. Simulation and measurement results have been done and showed that the antenna with DGS can improve the antenna performance of the antenna without DGS. This paper discusses the influence of hexagonal shape DGS towards the improvement of the radiation properties. By adding the DGS, therefore, will suppress surface wave propagation in the dielectric layer.

1.1.2. Antenna Design

A configuration of double hexagonal DGS implemented to the antenna is shown in Fig. 1.1. The antenna without DGS, as in [5], is designed on a single layer dielectric substrate with $\epsilon_r = 2.2$, thickness of 1.57 mm and tangential loss of 0.0009. The antenna is designed to have circular polarized bandwidth of minimum 50 MHz and resonant frequency at 2.61 GHz. Two element triangular microstrip antenna arrays with a distance between each element of 77 mm are fed asymmetrically to achieve tilted angle radiation pattern towards 30°. The stub is given for matching in the antenna without DGS and the Y slot in the triangular patch is inserted to excite circular polarization.

The DGS is then inserted into the ground plane of the antenna with position between the two element triangular patch, the DGS is drawn with dash lines to indicate that the DGS is located on the bottom of the substrate. The patch and the feeding system with stub from the antenna are not changed; only hexagonal shape slot is inserted to the ground plane of the antenna.

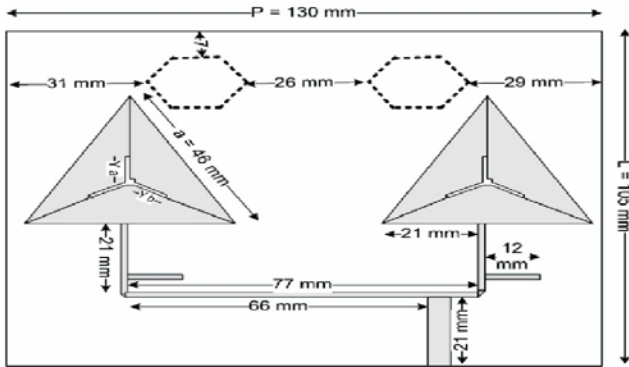


Fig 1.1

Figure 1.1. Configuration of double hexagonal DGS antenna design

The proposed hexagonal DGS design in this paper was simulated by varying the dimension and locating the position of the DGS on the antenna without DGS. The first simulation used one hexagonal DGS implemented to the antenna and showed no significant result. However, the best result shown for a single hexagonal is when the area of the hexagonal equals to 259 mm^2 with the side length of 14 mm. Therefore, based on the previous simulation, the next one is expanded to two hexagonal DGS with the total area of the DGS maintained at 259 mm^2 . The separation of one hexagonal to two hexagonal was carried out because it is assumed that the surface wave which has a zigzag path can be trapped by the two hexagonal instead of one. Therefore the hexagonal design was separated into two hexagonal. Finally, the double hexagonal shape DGS is designed between the two elements, in which the distance between the two elements as well as the location is varied. A good result was achieved for hexagonal with the side length of 10 mm and with the displacement between the two hexagonal of 26 mm.

1.1.3. Results and Discussion

1.1.3.1. Simulations

The simulation was carried out by using method of moment. Figure 1.2 exhibits the simulation result of the return loss of the antenna with and without DGS. The antenna with and without DGS has return loss of -43.22 dB and -33.3 dB at the resonant frequency of 2.61 GHz, respectively. The

simulation result of DGS shows return loss improvement of 29.8% compared to the antenna without DGS.

The triangular patch microstrip antenna array was designed to have circular polarization. The simulation result of the antenna with and without DGS for circular polarization shows a 3 dB axial ratio bandwidth of 2.6% and 1.9% respectively. This result shows that the antenna with DGS could increase the circular polarization bandwidth of the antenna without DGS to 10 MHz

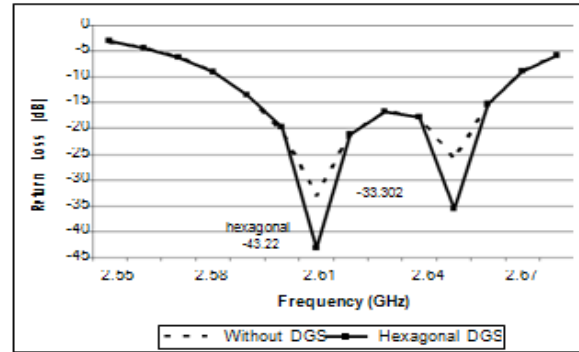


Fig 1.2

Figure 1.2 Comparison of simulated Return Loss between antenna with and without DGS antenna.

Another antenna parameter was also simulated, namely the mutual coupling. The simulation showed that the antenna without DGS has a mutual coupling of -39.68 dB and with DGS shows a reduction of mutual coupling to -41.84 dB which is 2.16 dB lower than the antenna without DGS. The simulation results showed that the antenna parameters of the antenna without DGS were improved by the DGS.

1.1.3.2. Measurements

The antenna with hexagonal DGS was fabricated and measured. The DGS antenna showed characteristic improvement compared to the antenna without DGS. The measurement results demonstrated that the hexagonal DGS antenna improved the impedance matching of the antenna without DGS from minimum return loss -30.18 dB to -40.89 dB . This means there is an improvement to 35% of the minimum return loss which can increase the efficiency of the antenna. This improvement is displayed in Figure 3.3. Figure 3.3 shows the measured resonant frequency of the antenna with and without DGS is at 2.66 GHz.

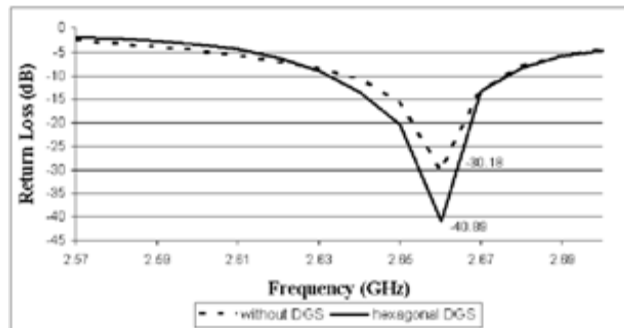


Figure 1.3 Measurement result of return loss.

There is a slight shift of resonant frequency from simulation compared to measurement results. However the measured result of the antenna with and without DGS shows the same resonant frequency, therefore this measured result can be compared.

For the circular polarization of the antenna, axial ratio bandwidth was measured. The result showed an increase of 3 dB axial ratio bandwidth of 10 MHz for the DGS antenna. The antenna without DGS has axial ratio bandwidth from 2.63 GHz to 2.67 GHz and the antenna with DGS from 2.63 GHz to 2.68 GHz.

Furthermore, the antenna gain was measured from 2.6 GHz to 2.7 GHz and the results are shown in Figure 1.4. It is shown that there is gain improvement of about 1 dB from the DGS antenna. This gain enhancement justifies the impedance matching result of the return loss, which proves that the efficiency of the antenna is also improved.

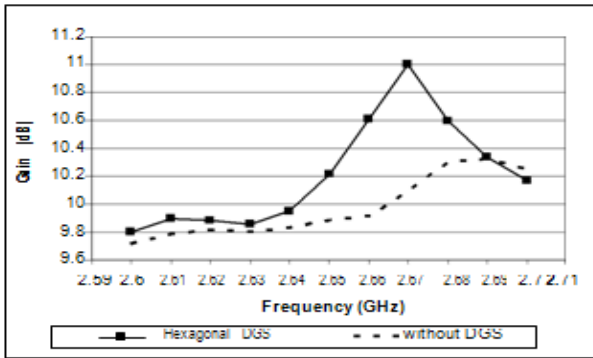


Figure 1.4 Comparison of measured gain between antenna with and without DGS.

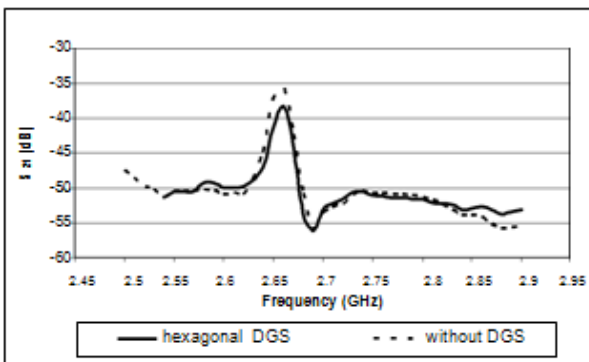


Figure 1.5 Comparison of measured mutual coupling between antenna with and without DGS.

Figure 1.5 shows the comparison of measured mutual coupling between the antenna without and with DGS. The measured mutual coupling results showed that the antenna with DGS has a mutual coupling of -38 dB at the resonant

frequency of 2.66 GHz, while the antenna without DGS has a mutual coupling of -35 dB. It is obvious from the result that there is a substantial mutual coupling reduction.

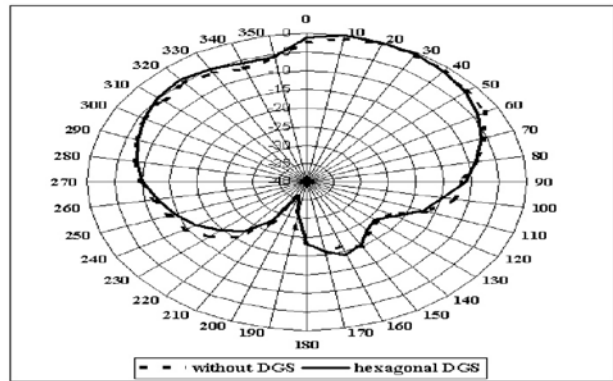


Figure 1.6 Measured *E*-plane radiation pattern of antenna with and without DGS.

Moreover, the measured radiation patterns of the antenna in the *E*- and *H*-plane for both with and without DGS are shown in Figure 1.6 & Figure 1.7, respectively. The antenna radiation patterns were measured at frequency 2.66 GHz. It is shown from Figure 1.6 that both antennas have similarity in the

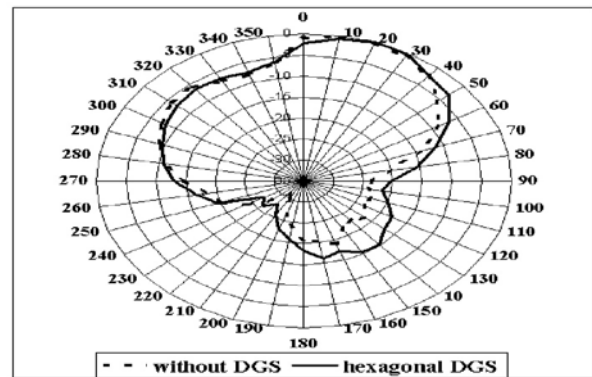


Figure 1.7 Measured *H*-plane radiation pattern of antenna with and without DGS.

E-plane pattern with maximum beam tilted towards 10° – 30° . This result agrees well with the intended design. While in Figure 1.7, the antenna with DGS has a slightly higher back lobe level in the *H*-plane due to the presence of the hexagonal defected structure acting as a slot antenna which causes leakage field distributions.

1.2. WIDE BAND TRIANGLE SLOT ANTENNA WITH TUNING STUB

1.2.1. Introduction

In applications where size, weight, cost, performance, ease of installation, and aerodynamic profile are constraints, low profile antennas like microstrip and printed slot antennas are required. Printed slot antennas fed by coplanar waveguide have several advantages over microstrip patch antennas. Slot antennas exhibit wider bandwidth, lower dispersion and lower radiation loss than microstrip antennas, and when fed by coplanar waveguide they also provide an easy means of parallel and series connection of active and passive elements that are required for improving the impedance matching, gain. Bow-tie and coplanar waveguide fed bow-tie slot antennas are planar-type variations of the biconical antenna that has wideband characteristics. A number of bow-tie slot designs are recently introduced which demonstrate wide bandwidth that ranges from 17% to 40%. However, in order to use these antennas in a phased array system, the antenna element size must be smaller than half the wavelength at the highest operating frequency to avoid grating lobes while scanning the main beam. Thus, the separation distance between elements must be small and such spacing results in high coupling, which causes scan blindness and anomalies within the desired bandwidth and scan volume. In this paper, a novel design of a small slot triangle antenna that supports the wideband characteristics of a bow-tie slot antenna and the low coupling characteristics between similar elements is presented. The radiation characteristics of the antenna versus its geometrical parameters are presented. The main beam direction of this antenna can be redirected 90 degrees off its original direction by simply etching the slot across two perpendicular conducting planes without loss of its main characteristics. The numerical simulation and analysis for this class of antennas are performed using the Momentum software package of the Advanced Design System (ADS) by Agilent Technologies. The ADS simulator, Momentum, is based on the solution of the mixed potential integral equations (MPIE) using full wave Green's functions for layered structures and the method of moment (MoM) technique. Verifications of the ADS results are further performed by using our developed finite difference time domain (FDTD) code supported by the CPML absorbing boundary, and by measurements of the return loss using the HP vector network analyzer 8510C.

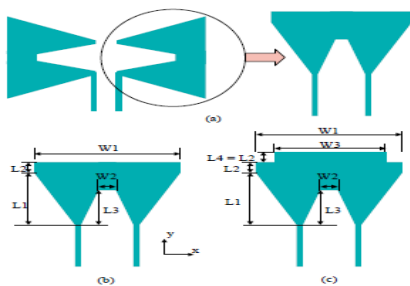


Figure 1.8 The proposed geometries of the triangle slot antennas with tuning stub. (a) Creating the geometry, (b) Initial design, and (c) Triangle slot with slot cap.

1.2.2. Antenna Geometry

The proposed geometries of the triangle slot antennas with tuning stub are shown in Figure 1.8. The first design is created by rotating half of a bow-tie slot antenna by 90°, and introducing a tapered metal stub and upper rectangular slot to tune the antenna, as shown in Figure 1.8. In the second design, we introduced a cap (hat) slot to improve the return loss level. As shown in Figure 1.8, W_1 is the width of the triangle, W_2 is the width of the upper width of the stub, W_3 is the width of the slot hat, L_1 is the height of the triangle, L_2 is height of the rectangular slot, and L_3 is the height of the tuning stub. The antenna is supported by a dielectric substrate of height equals to 32 mil and a relative dielectric constant of 3.38. The coplanar waveguide is designed for a 50Ω characteristic Impedance with slot and feed line widths equal to 0.15 and 2.61 mm, respectively

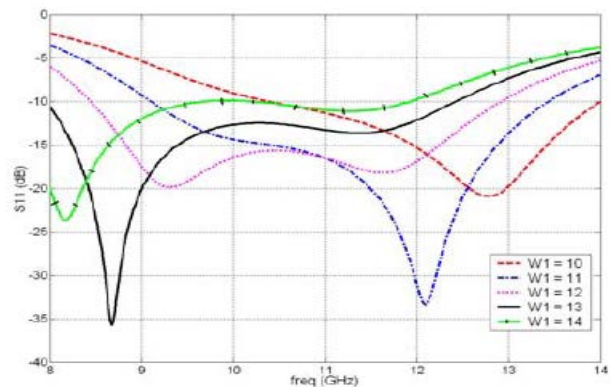


Figure 1.9 The effect of changing W_1 on the return loss

1.2.3. Parametric Study

In order to provide design criteria for this antenna, the effects of each geometrical parameter are analyzed. The parameters for the initial design of this antenna are studied based on ADS Momentum simulation results. The antenna dimensions (W_1 , W_2 , L_1 , L_2 and L_3) are chosen to be (12, 0.8, 8.5, 0.75 and 6mm) and one parameter is changed at a time while the others are kept constant. Figures 1.9, 1.10, 1.11, 1.12 & 1.13 show the effect of changing W_1 , W_2 , L_1 , L_2 and L_3 , respectively. All the results in these figures show that this antenna has two resonant frequencies. As shown in Figure 1.9, with the increase of W_1 the two resonant frequencies shift to slightly lower frequencies. While the W_2 variations, as shown in Figure 1.10, control only the level of the return loss at the two resonant frequencies without changing their values or the antenna bandwidth. Figures 1.11, 1.12 & 1.13 show that changing any vertical dimension (L_1 , L_2 and L_3) can improve the antenna impedance bandwidth. As shown in Figure 1.11 & 1.12, with the decrease of L_1 and L_2 , the lower resonant frequency shifts to a lower frequency, and the higher resonant frequency shifts to a higher frequency resulting in an increase of the antenna impedance bandwidth

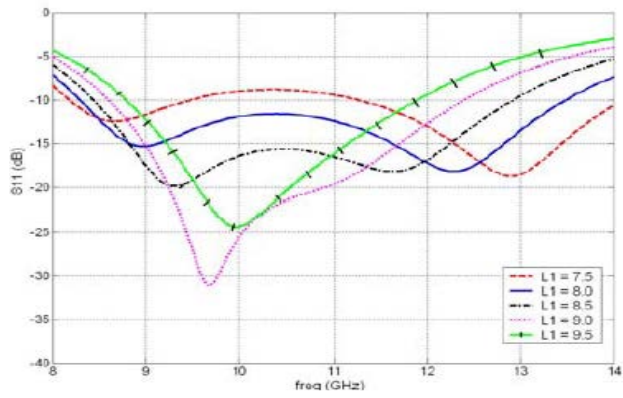


Figure 1.10 The effect of changing $W2$ on the return loss.

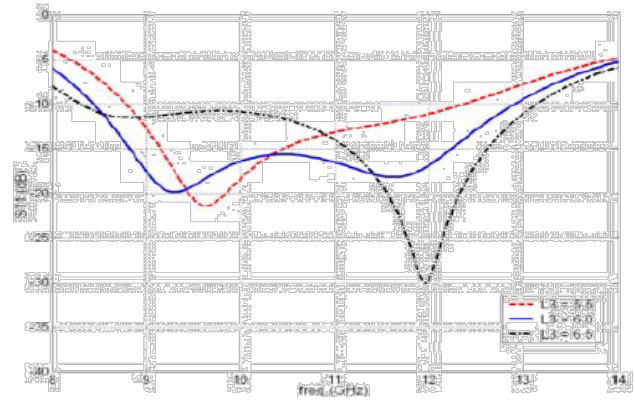


Figure 1.12 The effect of changing $L2$ on the return loss.

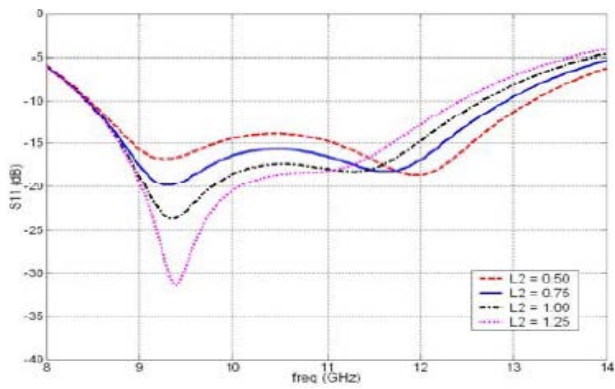


Figure 1.11 The effect of changing $L1$ on the return loss.

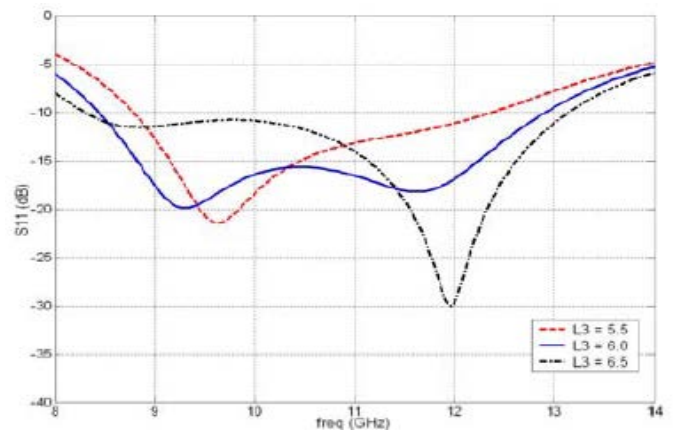


Figure 1.13 The effect of changing $L3$ on the return loss.

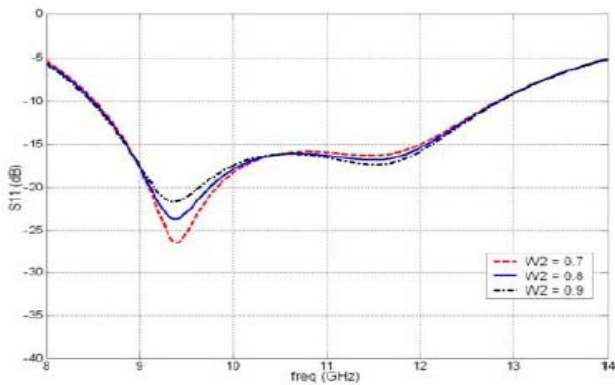


Figure 1.12 The effect of changing $L2$ on the return loss.

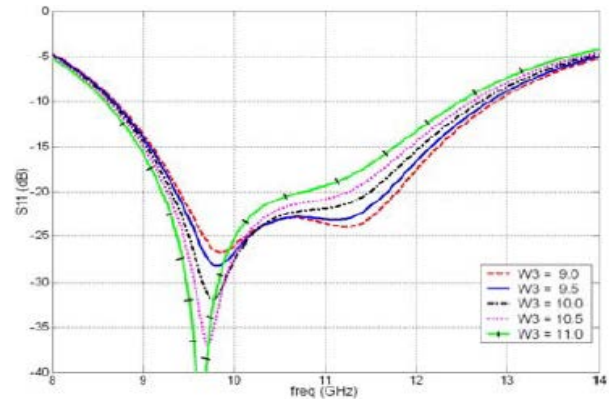


Figure 1.14 The effect of changing $W3$ on the return loss.

When the return loss level between the two resonant frequencies is less than -10 dB. On the contrary, as shown in Figure 1.13, with the decrease of L_3 the lower resonant frequency shifts to a higher frequency, and the higher resonant frequency shifts to a lower frequency. From the results of Figures 1.10 to 1.13, one may conclude that the most effective parameters for this configuration are W_1 , L_1 and L_3 . These parameters are calculated as functions of λL and λH ; the free space wavelength calculated at the lower and higher resonant frequencies, respectively. The outcomes of this analysis reveal that W_1 should be around $0.37 \lambda L$, L_1 around $0.33 \lambda H$ and L_3 around $0.25 \lambda H$. By adding a slot cap, as in the second design, we improved the return loss level to be less than -20 dB, and at the same time we maintained the overall impedance bandwidth, as shown in Figure 1.14. The height of the cap is kept equal to L_2 (0.75mm) and the effect of varying the cap width (W_3) is shown in Figure 1.14. The value of W_3 controls the return loss levels at the two resonant frequencies. As W_3 decreases the impedance bandwidth increases, however the operating band of the antenna shifts to higher frequencies.

1.2.4. Verification

A triangle slot antenna with tuning stub and a slot cap of ($W_1, W_2, W_3, L_1, L_2, L_3, L_4$) = (12.0, 0.8, 10.5, 8.5, 0.75, 6.0, 0.75mm) is simulated using our own developed FDTD code. The same antenna is fabricated and measured using the HP 8510C network analyzer. The ground plane is truncated at 1 cm away from the triangle slot. The computed return loss using the FDTD technique and ADS Momentum, and the measured return loss are depicted in Figure 1.15, where a very good agreement can easily be noticed. According to the measurements, the antenna operates from 8.1 to 13.45 GHz with around 50% bandwidth, which covers almost all the X-band and a part from the Ku-band.

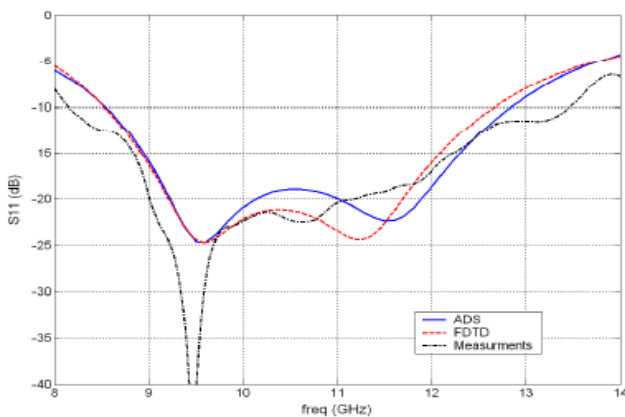


Figure 1.15 A comparison between the computed return loss using ADS

Momentum and FDTD, and the measured return loss for a triangle slot with tuning stub and a slot cap of $W_1, W_2, W_3, L_1, L_2, L_3$ and L_4 equal 12.0, 0.8, 10.5, 8.5, 0.75, 6.0 and 0.75 mm, respectively.

1.2.5. Radiation Property

ADS Momentum considers an infinite substrate even when the antenna has a finite ground plane and as a result it produces zero fields in the x-y plane. Therefore, we used the FDTD to compute the radiation pattern instead, and used ADS to calculate the gain and the directivity for an antenna with finite ground plane that is truncated at 1 cm distance from the triangle slot. The radiation patterns in the x-z (H-plane) and the y-z (E-plane) as well as the x-y plane at 10 GHz are shown in Figure 1.16. The antenna has an omni-directional pattern. The

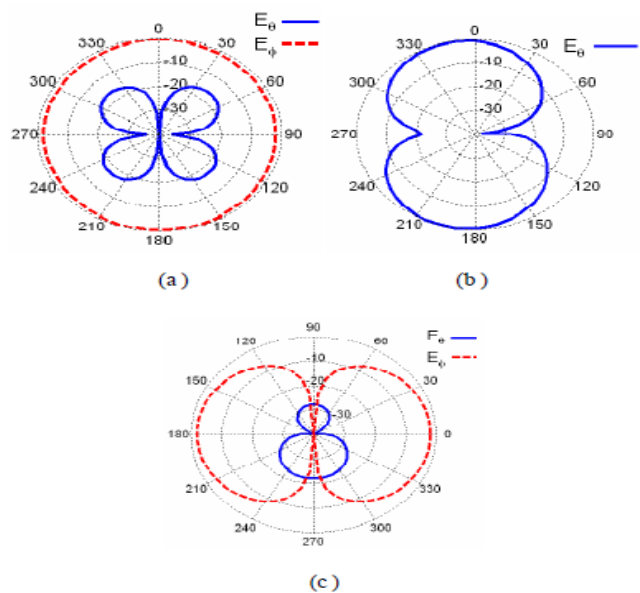


Figure 1.16 Radiation pattern at 10 GHz in the: (a) x-z plane (H-plane), (b) y-z plane (E-plane), and (c) x-y plane.

3.2.6. Antenna Arrays

Two elements of this antenna are simulated with a parasitic upside down triangle slot in between to decrease the coupling. The geometry and dimensions in mm of the two-element array are shown in Figure 1.18, while Figure 1.19 shows the coupling with and without the parasitic triangle slot, and the return loss in dB for two-element array. It is noticed that the coupling is less than -15 dB except in the range between 8 to 9 GHz, with a 2mm separation distance between the two elements.

This makes the antenna suitable for phased array systems because the edge-to-edge distance (d) as a function of λ_0 from 8 to 13GHz (d/λ_0) ranges from 0.37 to 0.6, which is considered optimum for narrow beamwidth and lowering

grating lobe requirements within this wide range of frequencies. Figure 1.20 shows that the main beam can be steered to 50° without grating lobes using only 8-element array.

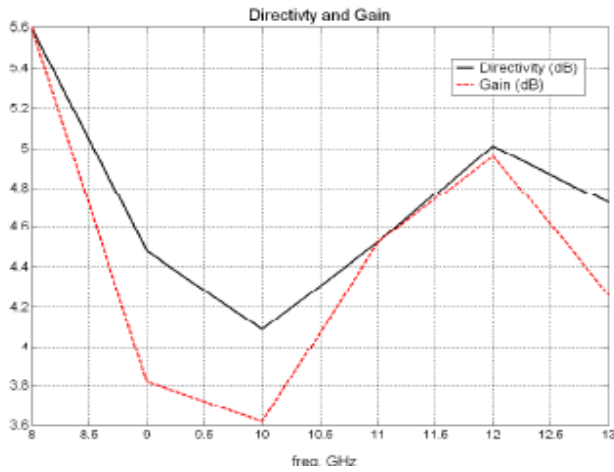


Figure 1.17 Computed gain and directivity as a function of frequency

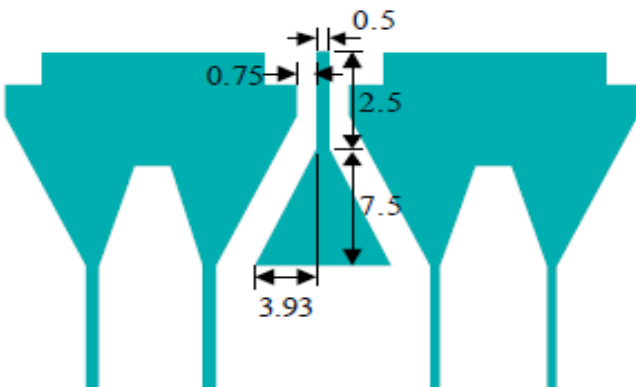


Figure 1.18 Geometry of two-element array of the triangle slot antenna with a separating upside-down triangle slot to decrease the coupling

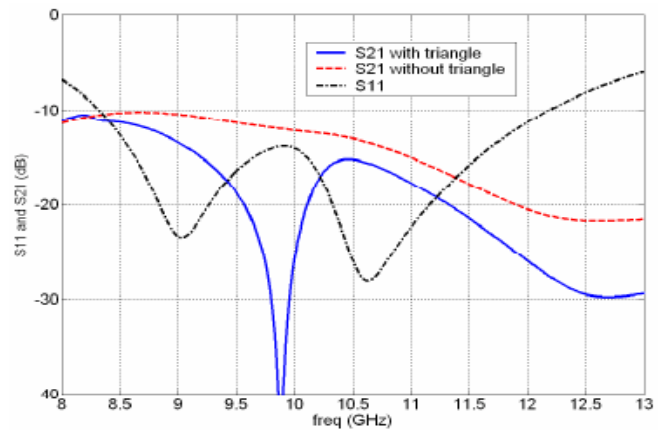


Figure 1.19 Return loss and coupling in dB for the two-element array

in Figure 1.18 with and without the upside-down separating triangle.

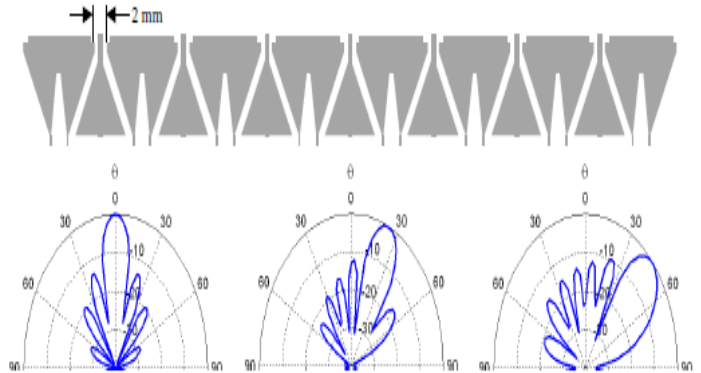


Figure 1.20 $E\phi$ in the x - z plane (H -plane) with 8-element array of the triangle slot antenna with tuning stub at 10 GHz, at a scanning angle of (a) 0° (b) 30° and (c) 50° .

1.2.7. Effect of bending the antenna

One approach to obtain radiation in the y -direction (end fire) for this type antenna is by making a 90° bend around the middle of the antenna. The geometry of the antenna after bending is shown in Figure 1.21, where the antenna is bent at the end of the tuning stub. One would then expect a figure of eight pattern for the $E\phi$ component

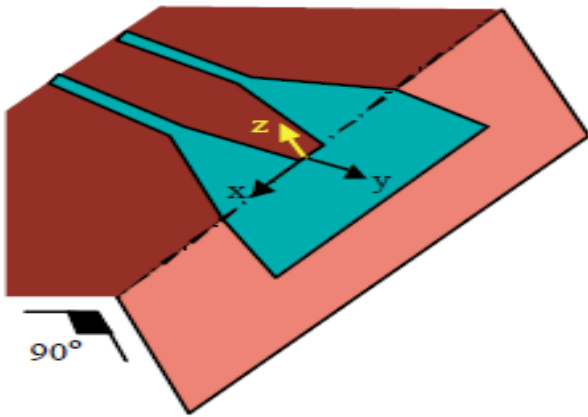


Figure 1.21 Geometry of the antenna after bending.

in the x - y plane (H -plane) with a resulting cross-polarized field. In the y - z plane (E -plane), we expect that the $E\theta$ would have a maximum at 90° because of the vertical field between the edge of the tuning stub and the lower edge of the triangle slot, in addition to two maximums at 0° and 180° because of the horizontal electric current in y -direction flowing in the tuning stub. Since there is no reason to have a null in between these maxima, one would expect a uniform $E\theta$ between 0° and 180° . At the same time, no cross polarization is expected because of the symmetry of the antenna.

The bent antenna is simulated using the FDTD code. The radiation patterns are shown in Figure 1.22, where the simulation results are confirming the expectations addressed in the above paragraph.

The cross polarization level in the x - y plane is -10 dB, relative to the copolarized field within the 3dB beamwidth area. A comparison between the computed return loss using the FDTD simulations after and before bending is shown in Figure 1.23, where one notices an increase in the bandwidth approaching 58%. A comparison between the measured return loss and the FDTD results is shown in Figure 1.24. According to the measurements, the bent antenna operates from 8.25 to 14.8 GHz with a return loss smaller than -10 dB, for a bandwidth of 57%.

1.2.8. Comparison with bow tie antenna

In order to demonstrate the advantages of this triangle slot antenna, it is worth comparing it with the class of printed and slot bow-tie antennas recently presented in [8–9]. This comparison will focus on

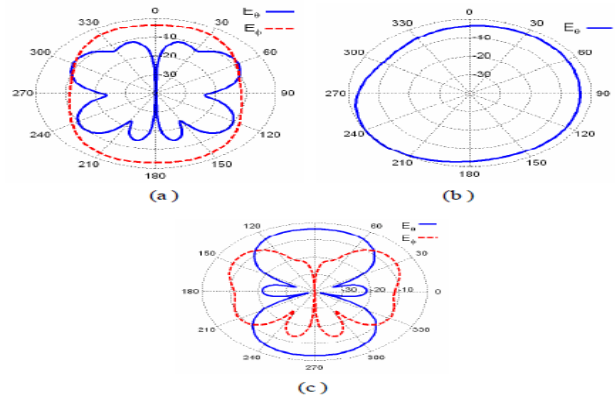


Figure 1.22 Radiation pattern at 10 GHz for the antenna after bending in the: (a) x - z plane, (b) y - z plane (E -plane), and (c) x - y plane (H plane).

The antenna size and impedance bandwidth. The bow-tie antennas available in the open literature provides a maximum bandwidth of 40% with antenna size equivalent to $0.4 \lambda_{0L}$ and $0.6 \lambda_{0H}$, where λ_{0L} and λ_{0H} are the free space wavelength calculated at the lower and upper limits of the operating frequency band of the antenna. The triangle slot antenna, designed in this paper, provides a bandwidth of 57% with size equivalent to $0.33 \lambda_{0L}$ and $0.54 \lambda_{0H}$. Consequently, the triangle slot antenna is smaller than the available printed and slot bow-tie antennas and it provides a wider bandwidth.

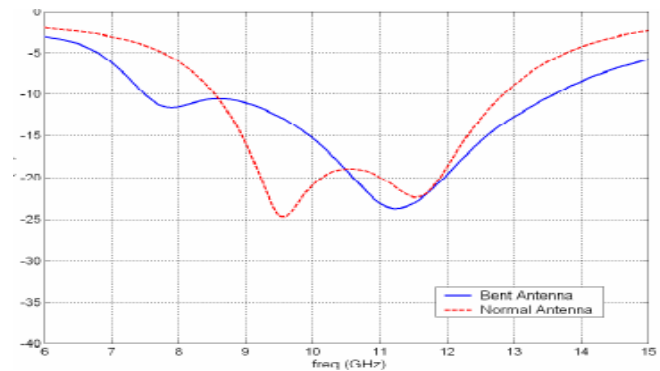


Figure 1.23 Comparison between the computed return loss of the antenna using the FDTD code after and before bending

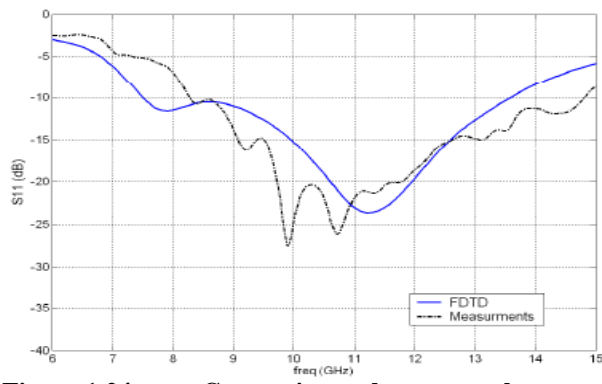


Figure 1.24 Comparison between the computed return loss of the bent antenna using the FDTD code and the measurement results.

A novel design of a small size triangle slot antenna with tuning stub is proposed and designed for wide band operation in the X-band. The effect of bending the antenna to obtain end-fire radiation has also been studied. This antenna shows a wide bandwidth (57%) and low cross polarization level in the E-plane and H-planes (-10 dB), and an average gain of 4.5 dB. These features exceeds those of available printed and slot bow-tie antennas. Low coupling between elements of this antenna in a linear array configuration is achieved with only 2mm separation distance. These characteristics make this novel, small size, triangle slot antenna suitable for being an element in a phased array system that requires wide bandwidth, high gain, small size, narrow beam width and large scanning capabilities.

V. CONCLUSION

A new DGS geometry, the double hexagonal shape have been used for two element triangular microstrip antenna array. The results demonstrated that the radiation properties of the antenna with DGS have better performance than the antenna without DGS. It is also shown that the geometry of the DGS has an influence towards the performance of the antenna characteristics.

A novel design of a small size triangle slot antenna with tuning stub is proposed and designed for wide band operation in the X-band. The effect of bending the antenna to obtain end-fire radiation has also been studied. This antenna shows a wide bandwidth (57%) and low cross polarization level in the E-plane and H-planes (-10 dB), and an average gain of 4.5 dB. These features exceeds those of available printed and slot bow-tie antennas. Low coupling between elements of this antenna in a linear array configuration is achieved with only 2mm separation distance. These characteristics make this novel, small size, triangle slot antenna suitable for being an element in a phased array system that requires wide bandwidth, high gain, small size, narrow beamwidth and large scanning capabilities.

REFERENCES

- [1] Yu, A. and X. Zhang, "A novel method to improve the performance of microstrip antenna arrays using dumbbell EBG structure," *IEEE Antennas and Wireless Propagat. Lett.*, Vol. 2, 2003.
- [2] Yang, L., Z. Feng, F. Chen, and M. Fan, "A novel compact EBG structure and its application in microstrip antenna arrays," *IEEE MTT-S Digest*, 1635-1638, 2004.
- [3] Salehi, M., A. Motevasselian, A. Tavakoli, and T. Heidari, "Mutual coupling reduction of microstrip antennas using defected ground structure," *10th IEEE International Conference on Communication Systems (ICCS)*, 1-5, Oct. 2006.
- [4] Zainud-Deen, S. H., M. F. Badr, E. El-Deen, K. H. Awadalla, and H. A. Sharshar, "Microstrip antenna with defected ground plane structure as a sensor for landmines detection," *Progress In Electromagnetics Research B*, Vol. 4, 27-39, 2008.
- [5] Rahardio.E.T., F.Y. Sulkily and M.Martin, "Design of circularly polarized equilateral triangular microstrip antenna array for satellite communication", Proc. of internat Symp. On antenna and propagation.(ISAP), Niigata, Japan, Aug.2007.
- [6] Liu, H., Z. Li, X. Sun, and J. Mao, "Harmonic suppression with photonic bandgap and defected ground structure for a microstrip patch antenna," *IEEE Microw. and Wireless Componets Lett.*, Vol. 15, No. 2, 55-56, Feb. 2005.
- [7] Chung, Y., S. Jeon, D. Ahn, J. Choi, and T. Itoh, "High isolation dual polarized patch antenna using integrated defected ground structure," *IEEE Microw. Component Lett.* Vol. 14, No. 1, 4-6, Jan. 2004.
- [8] Yu, A. and X. Zhang, "A novel method to improve the performance of microstrip antenna arrays using dumbbell EBG structure," *IEEE Antennas and Wireless Propagat. Lett.*, Vol. 2, 2003.
- [9] Yang, L., Z. Feng, F. Chen, and M. Fan, "A novel compact EBG structure and its application in microstrip antenna arrays," *IEEE MTT-S Digest*, 1635-1638, 2004.
- [10] Salehi, M., A. Motevasselian, A. Tavakoli, and T. Heidari, "Mutual coupling reduction of microstrip antennas using defected ground structure," *10th IEEE International Conference on Communication Systems (ICCS)*, 1-5, Oct. 2006.
- [11] Zainud-Deen, S. H., M. F. Badr, E. El-Deen, K. H. Awadalla, and H. A. Sharshar, "Microstrip antenna with defected ground plane structure as a sensor for landmines detection," *Progress In Electromagnetics Research B*, Vol. 4, 27-39, 2008.
- [12] Ang, B.K. and B.K.Chung, "A wideband microstrip patch antenna for 5-6 GHz wireless communication," *Progress In Electromagnetics Research*, PIER 75, 397-407, 2007.
- [13] *Microstrip and Printed Antenna Design*, Second Edition Randy Bancroft 300 pages SciTech Publishing, Copyright 2009
- [14] D. Liu and B. Gaucher, "Design Considerations for Millimeter Wave Antennas within a Chip Package," *IEEE International Workshop on Anticounterfeiting, Security, Identification*, pp. 13-17, April 2007.
- [15] Parui, Susanta Kumar, Moyra, Tamasi and Das, Santanu "Quasi-elliptic filter characteristics of an asymmetric defective ground structure," *International Journal of Electronics*, Vol.-96, No.-9, PP-915-924, September 2009